American Mineralogist, Volume 84, pages 400–406, 1999

Gillulyite $Tl_2(As,Sb)_8S_{13}$: Reinterpretation of the crystal structure and order-disorder phenomena*

Emil Makovicky† and Tonci Balić-Žunić

Geological Institute, University of Copenhagen, Øster Voldgade 10, DK 1350 Copenhagen K, Denmark

Abstract

The crystal structure of gillulyite $Tl_2(As, Sb)_8 S_{13}$ was reinterpreted based on the average structure determined by Foit et al. (1995). It consists of alternating PbS-like slabs comprised of As-S polyhedra and Tl-bearing slabs with partly zeolitic properties. In the latter, TlS_5 and As_2S_5 groups alternate regularly along the *b* direction and across the width of the slab, thus eliminating the need for S-S and As-As bonds postulated by Foit et al. (1995). These two types of slabs are also unit order-disorder (OD) layers, the ambiguities in stacking of which lead to several potential gillulyite polytypes. The actually observed OD phenomena are caused by ambiguity in the position of [010] TlS_5-As_2S_5 sequences (or of entire such layers), which can with equal probability assume two positions 1*b* apart.

Introduction

Gillulyite $Tl_2(As,Sb)_8S_{13}$ (As >> Sb) is the newest addition to the long line of Tl-As-Sb sulfosalts that have been identified since the first Tl-As sulfosalt, lorandite $TlAsS_2$, was described by Krenner in 1895. The description of gillulyite by Wilson et al. (1991) was followed by the crystal structure determination by Foit, Robinson, and Wilson in 1995. Many of the structural features of gillulyite reminded us of those in imhofite (Divjakovic and Nowacki 1976), which we reinterpreted as an OD structure (Balić-Žunić and Makovicky 1993). Closer study of the published gillulyite structure revealed that it, too, calls for reinterpretation in terms of OD theory. The new understanding of the crystal structure and OD character of gillulyite and its position in the crystal chemical system of sulfosalts are the principal topics of this contribution.

Structural units

Foit et al. (1995) described the crystal structure of gillulyite on the configuration level of strongly bonded units as composed of corrugated As-S and Tl-As-S (001) sheets that differ from one another by occupancy of a large coordination polyhedron by either Tl1 or an As4-As5-S7 group. For the latter configuration, As4 and As5 ought to be interconnected by a covalent As-As bond and the sheets themselves by S7-S7 covalent bonds (Figs. 4 and 5 in Foit et al. 1995). These two types of sheets should be intermixed in the structure of the mineral.

We describe the gillulyite structure on the next higher configuration level, taking into account also the weaker interactions, which ultimately keep the structure from collapsing, and refer to the structural similarities between gillulyite and several other sulfosalts with large cations. No existing structure drawing programs depict satisfactorily these configurations. The scheme used in the present paper requires more effort from the reader but gives better rewards; the scheme is compared to the approach used by ATOMS (Dowty 1993). On this higher level the gillulyite structure can be described as a parallel intergrowth of (1) Tl-containing ''A'' slabs with complex internal structure and partly zeolitic character with (2) $(011)_{PbS}$ ''B'' slabs of substantially distorted PbS archetype, with trapezoidal cross sections of coordination ''octahedra'' and periodic splitting of PbS motif on $(100)_{PbS}$ by additional As atoms on slab periphery. These slabs are parallel to $(001)_{gil}$ (Fig. 1).

PbS-like slabs

The B slabs of gillulyite are similar to the analogous PbS-based layers in gerstleyite $Na_2(Sb,As)_8S_{13}$. $2H_2O$ (Nakai and Appleman 1981) and in the synthetic compounds $(NH_4)_2Sb_4S_7$ (Dittmar and Schäfer 1977), $(N_2C_4H_8)Sb_4S_7$ (Parise and Ko 1992) and $(NC_2H_8)_2Sb_8S_{12}(S_2)$ (Tan et al. 1996). In all these Sb compounds, the same type of a generalized PbS-like $(011)_{PbS}$ slab occurs, with two alternating $(100)_{PbS}$ levels. One of them is two coordination polyhedra broad and periodically split by an additional Sb atom inserted in its periphery, whereas the other is a single $[011]_{PbS}$ row of trapezoidally distorted octahedra (Fig. 2). These two levels are periodically linked along the $[100]_{PbS}$ direction into strongly bonded double slabs by a number of short Sb-S bonds parallel to $[100]_{PbS}$; these are in turn separated by long Sb-S distances across the interspace filled with lone electron pairs of Sb (Fig. 3). This distribution of strong and weak bonds reminds us of the SnS structural archetype found in many sulfosalts (Makovicky 1997a) and in the case of $(NH_4)_2Sb_4S_7$

* We dedicate this contribution to the crystal chemistry of Tl sulfosalts no. 5 to our treasured friend and senior colleague, Charles Prewitt, on the occasion of his anniversary.

† E-mail: emilm@geo.geol.ku.dk

0003–004X/99/0003–0400$05.00

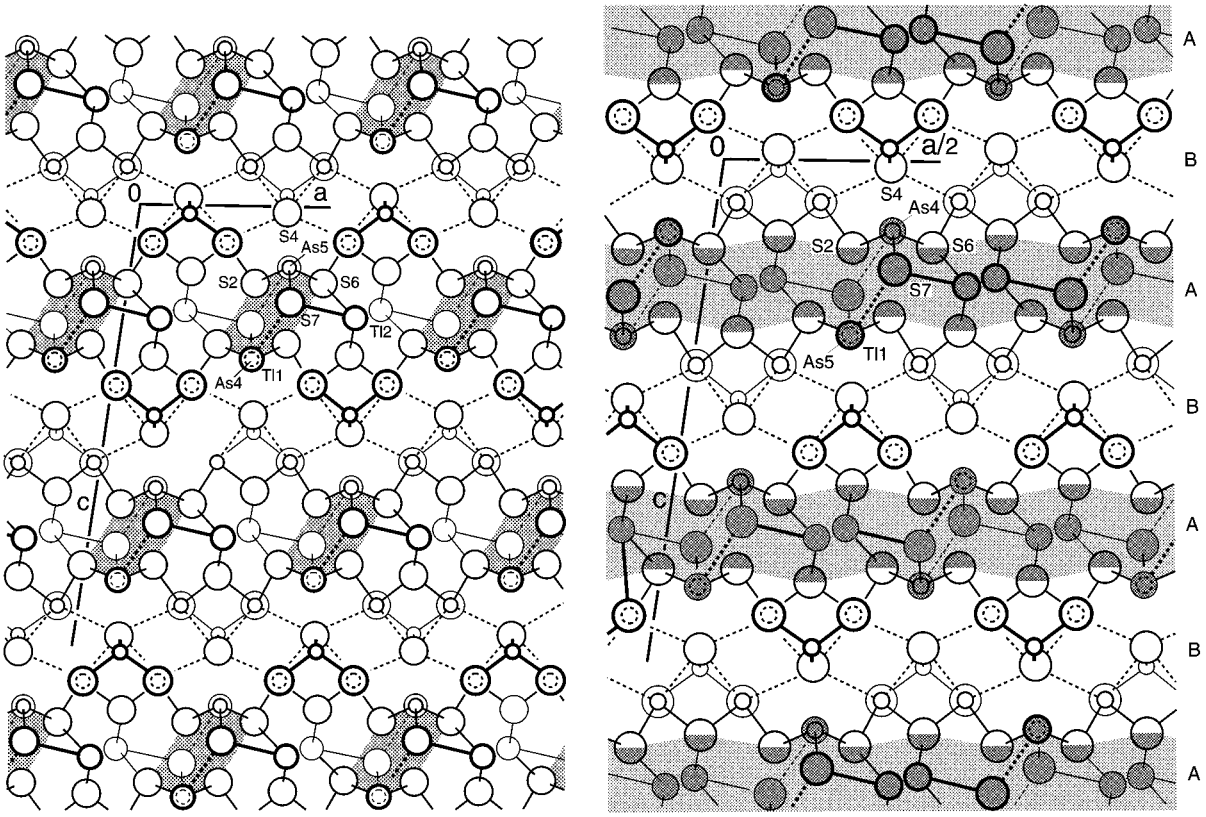

FIGURE 1. The crystal structure of gillulyite projected along [010]. In the order of decreasing size, circles denote S, Tl and (As,Sb). Line thickness indicates relative height above the projection plane. The A and B slabs indicated are defined in the text. Two ordered structure variants are shown, with the Tl1-As4 and As5 (and Tl2) ordering described as situations left and right in the text. Selected Tl1-As4 and As5 double rows are shaded. Tl2 positions are 50% occupied in both variants. Axis notation applies to the ordered variants.

the overall structure of B slabs is transitional between the PbS and SnS principles.

The B slabs in gillulyite do not follow the above principle of strongly bonded double layers. Distribution of strong and weak bonds along the $[001]_{PbS}$ direction in them is more complicated (Fig. 4) and, in addition, some $(100)_{PbS}$ levels are bound together by strong bonds in the immediately adjacent portions of A slabs. A similar principle is found in the PbS-based slabs of Pb-rich chabourneite $Tl_8Pb_4Sb_{21}As_{19}S_{68}$ (Nagl 1979). The PbS structure is substantially distended along $[100]_{PbS}$ in order to accommodate the active lone electron pairs of As in its interior as well as the large Tl polyhedra and the As_2S_5 groups on its periphery.

On the configuration level of the strongest, shortest bonds, close similarity exists between gillulyite and the above quoted structures. Loop-branched sinuous chains of AsS_3 (or SbS_3) polyhedra run along the edges of the PbS-like B slabs (Fig. 5). The chains are topologically identical for all these compounds except for chabourneite. Inside the B slab, these chains are glide-plane related in gerstleyite and the synthetic Sb sulfosalts, whereas they are related through a two-fold screw axis in gillulyite (for most structures these are only the local symmetry elements). This simple picture is complicated by further polymerization of these chains, which takes place through the A slabs and yields double chains in gerstleyite and $(NC_2H_8)_2Sb_8S_{12}(S_2)$. In gillulyite (argued in more detail below) these chains are paired in a different way: They form double-chains in the same B-slab, being interconnected by As_2S_5 groups on the slab margins.

Tl-containing slabs

The A slabs in the average structure of gillulyite display clusters of mutually incompatible atoms: 0.5 Tl1, 0.5 (As,Sb)4, 0.5 (As, Sb)5, and 0.5S7. This problem was resolved by Foit et al. (1995) as a mixture of two sheet types, one with Tl1, the other with As4-As5 pairs; the possibility of partial ordering of all the above atoms has been left open.

Considering the doubling of *b* direction suggested by weak/diffuse superstructure reflections (Foit et al. 1995) and our past experience with imhofite (Balić-Žunić and Makovicky 1993), we propose an alternative model for the A slabs, i.e., for the Tl1, As4, and As5 sites in gillulyite.

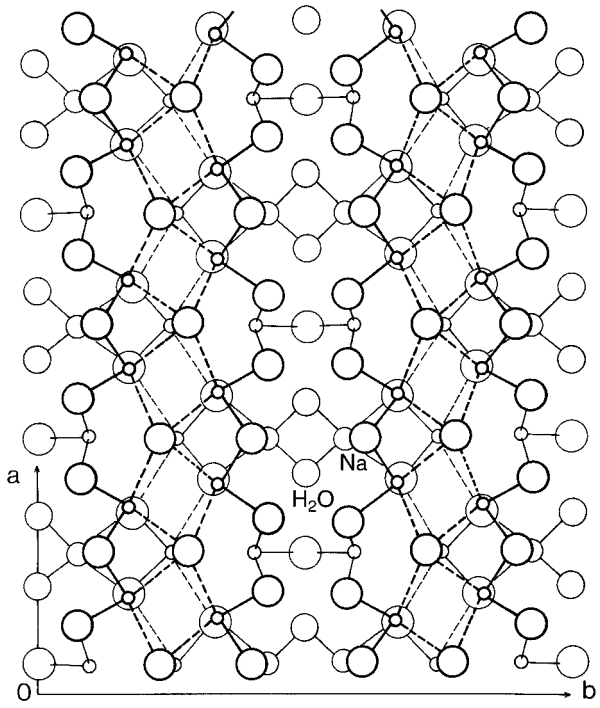

FIGURE 2. A two-layer thick slab from the crystal structure of gerstleyite $Na_2(Sb, As)_8S_{13}\cdot 2H_2O$ (Nakai and Appleman 1981). In the order of decreasing size circles denote S, H_2O, Na, and (Sb, As). Line thickness denotes height levels above projection plane (001).

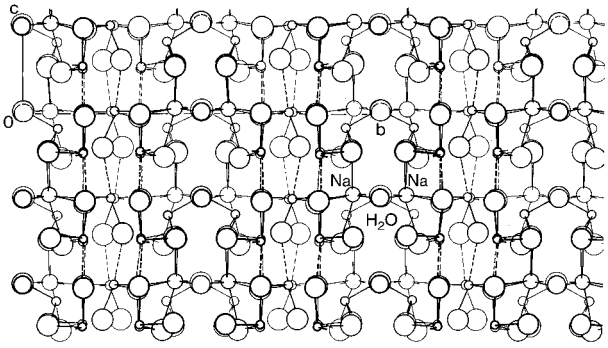

FIGURE 3. The crystal structure of gerstleyite projected along [100]. For symbols, see Figure 2.

Instead of being situated in separate sheets in the structure, the Tl1 sites and the As4 and As5 groups alternate regularly along each [010] row of the A slab (Fig. 4). In this interpretation, Tl1 is coordinated by an additional sulfur atom, S7, from the immediately adjacent [010] Tl1-As4 and As5 row. The same S atom is shared by the pair of As coordination polyhedra As4-As5 in this adjacent row (Figs. 1 and 4). The two rows are tied together by the array of common S7 atoms into a double row that is attached to the adjacent B slabs by common S2 and S6 atoms (Fig. 1). The *b* period of the A slab is twice that of the B slab due to the alternation of Tl1 and As4 with As5 polyhedra/groups in the [010] rows of the A slab. Between two adjacent double rows, a split and partly occupied Tl2 position is situated in the A slab; each of the split sites shows short Tl-S bonds to only one of these double rows (Fig. 1).

Two orientations are possible for the Tl1-As4 and As5 double rows adjacent along [100] in an A slab: (1) Tl1 in one double row is facing the As4 and As5 pair with the same *y* parameter in the adjacent double row (Fig. 1, left); (2) Tl1 and Tl1 or As4 and 5 and As4 and As5 with the same *y* parameters in the adjacent double rows face each other (Fig. 1, right). This in turn determines the behavior of Tl2.

The split Tl2 position appears to prefer strongly the shortest Tl2-S7 bond, suggesting that the As4-As5 pair in the [010] double row should be on the side oriented toward the nearby Tl2 atom. The adjacent [010] double row, on the opposite side of this Tl2 atom, will be on its far side and its exposed cation should be Tl1, i.e., the first model. This will force all Tl1 atoms with the same y_A parameter to be on the same side of the A layer with all As4 and As5 groups being on its opposite side. Tl2 will fill the channel statistically and in a zigzag fashion, 0.5 Tl at each *y* level (Fig. 1, left).

The second case involves ordering of Tl2 atoms at those *y* levels where they are sandwiched between S7 atoms of the As4-As5 groups, which are situated on both sides of Tl2. Tl2 will be absent from those levels, $\Delta y_A = 0.5$ away, where Tl1 atoms line the Tl2 channel. At these y_A levels, it is the adjacent Tl2 channels that are lined by As4-As5 groups with S7 and occupied by Tl2. This model accounts quite naturally for the half-occupancy of the Tl2 position obtained in the refinement by Foit et al. (1995), which makes it the preferred alternative, but it has to tolerate its statistical splitting and fluctuations on every occupied level (Fig. 1, right). In contrast, the first model orders Tl2 into only one of the split positions but has to tolerate the statistical half-occupancy of Tl2, which in this model is not caused by the nature of the Tl2 position but by the overall stoichiometry of the phase. Both alternatives give the same average structure; only the superstructure reflections will differ. No apparent reason exists for correlation between the Tl1 (As4 and As5, respectively) positions in the two [010] double rows separated by the B slab.

Neither S-S nor As-As bonds exist in the new model: S7 is always sandwiched between one Tl1 atom and one As4 and As5 group, with perfectly appropriate distances of respectively 3.302 Å and 2.296 or 2.299 Å. With every second S2-S2-S6-S6 rectangle being occupied by Tl1, the As4 and As5 polyhedra are paired above one rectangle (Fig. 4) and not across the boundary of two such rectangles as suggested by Foit et al. (1995). Therefore, the non-crystallographically oriented As-As bond, not coincident with any of the three p^3 bonds (cf. realgar; Mullen and Nowacki 1972) becomes superfluous. As4 and As5 form a pair of three-fold pyramids with S7 in common

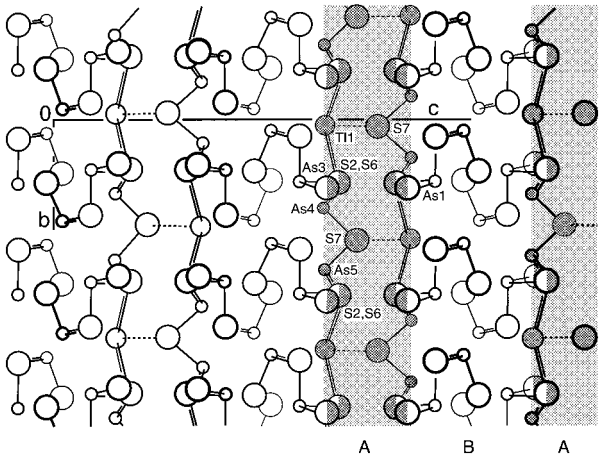

FIGURE 4. The crystal structure of gillulyite projected along [100] with the A and B slabs indicated. For symbols, see Figure 1.

and the space for their lone electron pairs is defined by the ''wedge'' S2-S4-S6 inserted into the PbS-like motif of the B slab.

THE PHENOMENON OF ORDER-DISORDER POLYTYPISM

Order-disorder structures (Dornberger-Schiff 1956) are a special subgroup of polytypic structures. According to the official definition (Guinier et al. 1984), polytypes are structures built up by stacking layers of identical structure and composition; distinct polytypes differ by their stacking sequence. In the OD structures (polytypes), the ambiguity in layer stacking modes allowed by this definition is reduced in such a way that all layer pairs are equivalent, whereas layer triples, quadruples, etc., are not equivalent; these become equivalent in the special cases of so-called maximum degree of order (MDO) sequences, i.e., standard polytypes. Besides the polytypes with MDO or more complicated periodic layer stacking sequences, nonperiodic random stacked sequences also occur.

All OD polytypes from one OD family have a set of sharp diffractions in common—the so-called family diffractions—and another set of diffractions that are characteristic for the given polytype; for disordered sequences, the latter turn into diffuse reflections.

The unit layers of OD structures are not crystal chemical units, but they are geometric units selected in such a way that they allow geometric ambiguity of stacking on their boundaries while preserving the nearest neighbor coordinations on this boundary (i.e., the equivalence of layer pairs). OD structures can be built from one, two, or more kinds of unit layers. Each layer has its own symmetry group; they can be polar or non-polar. A convention has been introduced of placing the symmetry axes perpendicular to (symmetry planes parallel to) the unit layers in round brackets in the layer group symbol.

For OD structures based on one kind of layer, additional symmetry elements exist relating $(n+1)^{st}$ layer to the nth layer. For those compounds with two or more kinds of unit layers, translations describing the sequence of origins of consecutive layers in the OD layer pack is added.

Number Z of possible equivalent positions of the $(n+1)^{st}$ layer after the nth layer is obtained by dividing the multiplicity, N, of the subgroup of those symmetry operations in one layer, which are not reversing this layer by the multiplicity, F, of these operations valid for the layer pair in question ($Z = kN/F$, $k = 1$ or 2; the so-called NFZ relation). Distinct Z values can result for distinct types of interfaces in a polytype.

Real OD polytypes always show deviations from ideal OD symmetry; the more ordered they are, the larger are these deviations. This phenomenon is called desymmetrization of OD structures. The closer the OD structure is to its ideal OD symmetry, the greater is its tendency to polytypism and disorder.

The best contemporaneous introduction to OD theory and OD polytypes is the review by Ďurovič (1997) on which this short account is based and papers in Merlino (1997). OD polytypism is not an exotic phenomenon: For example, it describes polytypism in close-packed metals, ZnS (SiC) polytypes, wollastonite polytypes, polytypism in micas, chlorites, serpentinite and kaolinite groups, saphirine-aenigmatite, pinakiolite family, and pumpellyite family (Merlino 1997). It also applies to gillulyite, imhofite, and several other sulfosalts of Tl-As, Cu-As, Pb-Sb, and Ag-Pb-Bi.

THE OD CHARACTER OF GILLULYITE

Gillulyite is an OD structure comprised of two types of unit layers, coincident with the A and B slabs of the

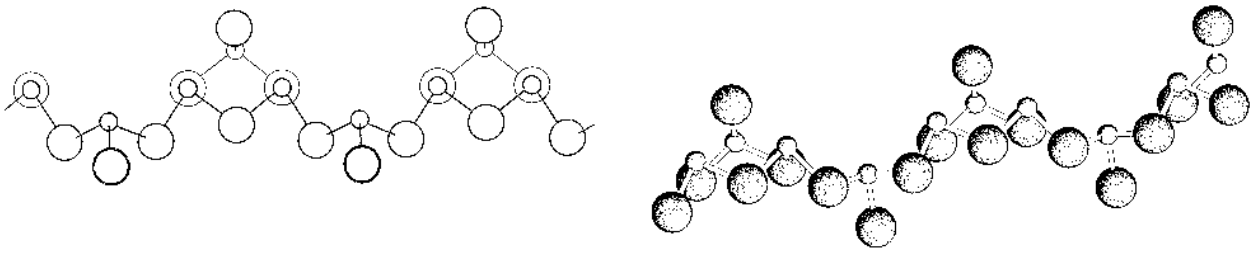

FIGURE 5. The tightly bonded loop-branched $(As, Sb)_4S_7$ chain present in the structures of gillulyite, gerstleyite and the synthetic Sb sulphosalts. Typified by the As4 containing chain [left; line thickness indicates three height levels for (As, Sb) and S atoms] and the As5 containing chain (right; drawn by ATOMS) in gillulyite.

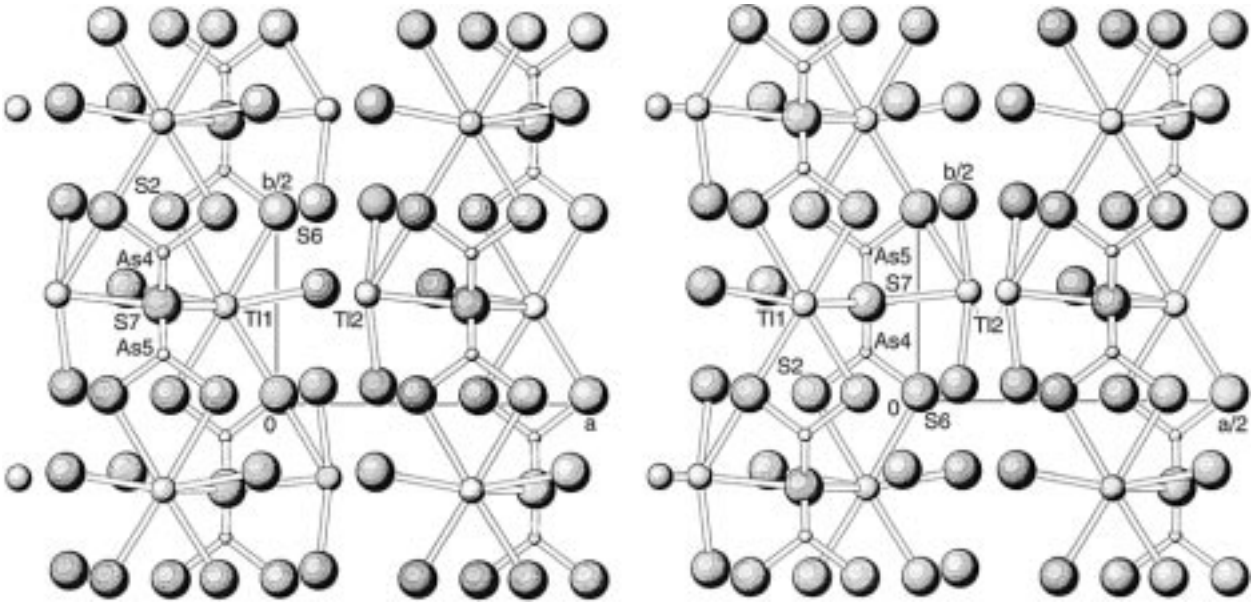

FIGURE 6. The A slab in gillulyite projected on (001). Circles in order of decreasing size denote S, Tl, and (As, Sb). Left, the ordered (**a**) variant of A slab with slightly idealized layer group symmetry $P12_1/m(1)$. Right, the ordered (**b**) variant of A slab with the slightly idealized layer group symmetry $C12/m(1)$. Drawn by ATOMS.

structure. The PbS-like B layers have symmetry $P2_1/m1(1)$, the *b* axes of the layer and of the unit cell coinciding. As4, As5, S7, Tl1, and Tl2 do not belong to these layers (Fig. 1). In the substructure, the A layers have layer group $P12/m(1)$ and the mesh based on the substructure periodicities. The situation is different for the two possible true structures of the A layer with the doubled *b* dimension. For the case with all Tl1 sites being on one and the same y_A level on the same side of [010] double rows, the A layers have layer group $P12_1/m(1)$ (Fig. 6, left); for the case with Tl2 sandwiched between adjacent As4-As5 groups on the same y_A level they have $C12/m(1)$ (Fig. 6, right).

According to the NFZ relationship (Ďurovič 1997), two equivalent positions can exist for an A layer after a B layer in the substructure. The monoclinic substructure cell inside a single A layer can be right- or left-handed, its β angle being defined as the angle between the cell axis *a* and the vector S2-S6 across the A layer.

Two equivalent positions are possible for the B layer after the A layer, either obeying the 2_1 axis in A, which is parallel to [010] and based on the b_A period, or obeying the symmetry centers in the A layer. The structure found by Foit et al. (1995) follows the first alternative, and the atomic planes (010) follow a slightly wavy course through the structure (Fig. 4). For the first alternative, the short [010] As-S vectors for As1 and As3 in two adjacent B slabs are parallel, for the second alternative they are antiparallel.

Altogether, four fully ordered combinations are possible of the A and B unit OD layers in gillulyite substructure: First, the $(2)_A$ and $(\bar{1})_B$ combination yields the subcell of gillulyite as described by Foit et al. (1995) i.e., $\mathbf{a} = \mathbf{a}_{gil}$, $\mathbf{b} = \mathbf{b}_{gil}$, $\mathbf{c} = \mathbf{c}_{gil}$, $\beta = \beta_{gil}$, and the substructure space group is $P2/n$. Second, the $(\bar{1})_B$ and $(\bar{1})_A$ combination yields a triclinic subcell with $\mathbf{a} = \mathbf{a}_{gil}$, $\mathbf{b} = \mathbf{b}_{gil}$, $\mathbf{c} = \mathbf{a}_{gil}/2 + 0.129\mathbf{b}_{gil} + \mathbf{c}_{gil}/2$ and space group $P\bar{1}$. Third, the $(2)_A$ and $(2_1)_B$ combination results in an orthorhombic subcell with $\mathbf{a} = \mathbf{a}_{gil}$, $\mathbf{b} = \mathbf{b}_{gil}$, $\mathbf{c} = (\mathbf{d}_{001})_{gil}$, and space group $P2_122_1$. Fourth, the $(\bar{1})_A$ and $(2_1)_B$ combination gives a monoclinic subcell with $\mathbf{a} = \mathbf{a}_{gll}$, $\mathbf{b} = \mathbf{b}_{gil}$, $\mathbf{c} = (\mathbf{d}_{001})_{gil} - 0.258\mathbf{b}_{gil}$ and space group $P2_1/c$. See Table 1 for values of these parameters. The $\bar{1}$ operator in the B layers produces the A layer orientations with always the same sense of intralayer β_A angle throughout the layer stack. The 2_1 operator in the B layers produces alternating orientations of this angle. Similarly, the $\bar{1}$ operator in the A layers gives the same sense of the intralayer α_B angle for the entire layer stack, whereas the 2 operator in the A layers yields alternating orientation of this angle. The γ angle is equal to 90° because of the layer configurations.

For each of the maximally ordered variants of the substructure further complications arise by ordering of the Tl1-As4 and As5 double rows in the A layers which also alter at least one subset of two-fold axes in these layers into 2_1 axes. In the true structure, each of the two orientations of the cell of the A layer can have Tl1 either at $y = 0$ or at $y = 0.5$ of the two-tier A cell. Moreover, they either yield the *P* or the *C* ordering variant of this cell. Due to 2_1 axes parallel to [100] in the B layer, the cell in the A layer is shifted by $1/2a$ after each B layer.

For example, the crystallography of the Tl-As ordered variants of the $(2)_A$ and $(\bar{1})_B$ substructure differs according to the Tl-As ordering in every second A slab. The simplest maximally ordered cases are as follows.

For the *P* type of ordering in the A slabs and every

TABLE 1. Crystal data for gillulyite, imhofite, and potential gillulyite polytypes

Phase polytype	Space group	*a* (Å)	*b* (Å)	*c* (Å)	α (°)	β (°)	γ (°)	Reference
Gillulyite $(2)_A$ and $(\bar{1})_B$†	subcell: $P2/n$	9.584	5.679	21.501	90	100.07	90	Foit et al. 1995
Gillulyite $(1)_A$ and $(1)_B$†	subcell: $P\bar{1}$	9.584	5.679	11.003	86.18	74.65	90	this work
Gillulyite $(2)_A$ and $(2_1)_B$†	subcell: $P2_122_1$	9.584	5.679	21.170	90	90	90	this work
Gillulyite $(1)_A$ and $(2_1)_B$†	subcell: $P2_1/c$	9.584	5.679	21.221	93.96	90	90	this work
Gillulyite *P*-ordering‡	cell: $P2_1/n$	9.584	11.358	21.501	90	100.07	90	this work
Gillulyite *C*-ordering‡	cell: $C2/c$	19.168	11.358	21.956	90	105.38	90	this work
Imhofite subcell§	subcell: $P2_1/n$	8.755	24.425	5.739	90	108.38	90	Divjaković and Nowacki 1976

† Data for real or hypothetical gillulyite subcells.
‡ Data for unit cells of selected ordered variants of the gillulyite polytype $(2)_A$ and $(\bar{1})_B$.
§ $a_{gil} \| b_{imh}$, $b_{gil} \| c_{imh}$; cell: $c_{imh} = 2c_{sub\text{-}imh}$.

second A slab with the same y_A height of Tl1, $\mathbf{a} = \mathbf{a}_{gil}$, $\mathbf{b} = 2\mathbf{b}_{gil}$, $\mathbf{c} = \mathbf{c}_{gil}$, and $\beta = \beta_{gil}$ and the space group is $P2_1/n$. This situation remains valid without regard to which one of the two possible y_A heights the Tl1 atoms in the odd A slabs assume. For the two alternative heights of the odd A slabs, two alternative subsets of symmetry elements from the substructure space group $P2/n$ will be used.

For the *C* type of Tl-As ordering in the A slabs, the simple maximally ordered variant results from the shift of every second A slab by a half of the true *b* parameter (i.e., by the width of one polyhedron) when we relate to the reference framework of gillulyite sublattice. Then $\mathbf{a} = -2\mathbf{a}_{gil}$, $\mathbf{b} = 2\mathbf{b}_{gil}$, and $\mathbf{c} = \mathbf{a}_{gil} + \mathbf{c}_{gil}$ for its unit cell. Both possible shifts for the odd A slabs, by either $\Delta y_A = 0.0$ or 0.5, give the same space group symmetry, $C2/c$ in terms of the new cell. Again, two alternative subsets of symmetry elements from the substructure space group $P2/n$ will be used in these two cases.

In both categories, other Δy_A shifts for even A slabs will give more complicated, centered unit cells. Only further research will show whether the OD phenomena proposed for gillulyite in this contribution act without restrictions or whether there is a partial desymmetrization of the real structure of OD layers (Ďurovič 1997), which in turn leads to a strong preference for certain maximally ordered structural variants both on the substructure and complete structure levels.

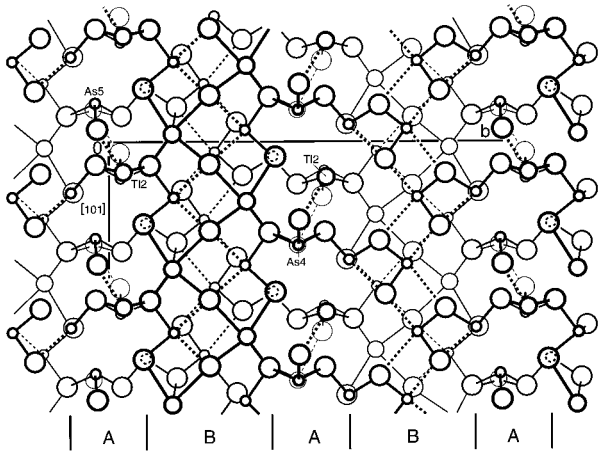

FIGURE 7. The crystal structure of imhofite $Tl_3As_{7.66}S_{13}$ (Divjaković and Nowacki 1976) projected along [001]. The A and B slabs are defined in the text. For conventions see Figure 1.

COMPARISON WITH IMHOFITE

Imhofite (Divjakovic and Nowacki 1976) is a monoclinic mineral with a pronounced subcell that has metrics superficially similar to gillulyite (Table 1). The projection of the imhofite structure along $[101]_{sub}$ (Balić-Žunić and Makovicky 1993, Fig. 6) shares a number of features with the projection of the gillulyite structure along [001] (Figs. 1, 2, and 3 in Foit et al. 1995) the strong and weak As-S bonds in the SnS-like B slab of imhofite appear to be copied in this projection by the PbS-based B slabs of gillulyite, whereas the A slabs contain the same $Tl1_{gil} \equiv Tl2_{imh}$ and As4 and As5 configurations in both phases. The presumed A portion in this projection of gillulyite (Figs. 1–3 of Foit et al. 1995) is by ½ coordination polyhedron narrower than in imhofite. This is in agreement with the difference of 5.275 Å between $2a_{gil} = 19.168$ Å and $b_{imh} = 24.425$ Å and the near identity of $b_{gil} = 5.679$ Å with $d(10\bar{1})_{imh} = 5.400$ Å. However, the similarity ends there: As seen in Figure 1, the next lower Tl1-As4 and As5 configuration in gillulyite is situated half-way between the previous Tl1-As4 and 5 double rows with no continuous interspace between them. Each Tl1-As4 and As5 double row is flanked by Tl2 channels after which the motif is shifted by 1/2 polyhedron to the right or left along $[100]_{gil}$. In terms of the Foit et al. (1995) description, considerable similarities apparently exist between gillulyite and imhofite within bounds of an individual tightly bonded [001] sheet of gillulyite structure, but they disappear in the way these sheets are stacked.

The Tl1-As4 and 5 double rows are a feature common for both structures. However, in exactly that direction in which they stack in imhofite—thus forming the A slab—they are separated by the PbS-like slab in gillulyite. In the direction orthogonal to the former one these double rows are separated by SnS-like slabs in imhofite but they form the A slabs in gillulyite in which they are separated only by Tl2 containing channels (Figs. 1 and 7). In the

A layers of imhofite, the adjacent double-rows are shifted by a half-width of coordination polyhedron resulting in the OD phenomena described by Balić-Žunić and Makovicky (1993). Considering individual double-rows, it is the same structural direction in which the OD phenomena in gillulyite also take place. This time, however, the rows involved are in consecutive A layers and the shifts are by a full-width of coordination polyhedron.

In both structures, all Tl1-As4 and As5 double rows have the same orientation in one A slab, thus defining the sense of the β_A angle. In imhofite, the structure of B slabs causes reversal of the sense of β_A in alternative A slabs. In the gillulyite structure determined by Foit et al. (1995), all A slabs have the same sense of β_A but the above specified OD phenomena should allow its reversal as well.

Position in the sulfosalt system

Gillulyite belongs to the family of sulfosalts with structures in which slabs derived from SnS- or PbS-archetype alternate with slabs of more complex structure; the latter serve as a vehicle for accommodation of large cations and/or active lone electron pairs. This family was first defined by Makovicky (1989) and enlarged by Makovicky (1997a) under the name of merotypes of hutchinsonite. (Merotypes are the structures composed of two alternating layer types in which one set of layers are isotypic, homeotypic, or homologous over the entire family, whereas the intervening layers may substantially differ between distinct members of the family. Makovicky 1997 b.)

In the light of present investigation, gillulyite $Tl_2(As,Sb)_8S_{13}$, gerstleyite $Na_2(Sb, As)_8S_{13}\cdot 2H_2O$, and the above-mentioned organic Sb sulfosalts with slabs based on PbS archetype (in which allowances have been made for a more active role of lone electron pairs) constitute one branch of this broad family. Imhofite $Tl_3As_{7.66}S_{13}$, hutchinsonite $TlPbAs_5S_9$, bernardite $TlAs_5S_8$, edenharterite $PbTlAs_3S_6$, jentschite $TlPbAs_2SbS_6$, pääkkönenite $Sb_2(As_{0.84}Sb_{0.16})S_2$, and kermesite Sb_2S_2O belong to the other branch in which one set of slabs is based on SnS archetype; the configurations in these slabs are designed to accommodate active lone electron pairs. In these two groups, respectively $(011)_{PbS}$ and $(010)_{SnS}$ configurational slabs are present. This is quite unlike the $(100)_{PbS}$, $(111)_{PbS}$, $(311)_{PbS}$ (lillianite homologues), $(501)_{SnS}$, or $(301)_{SnS}$ (sartorite homologues and the related Tl-As-Sb sulfosalts) slabs in diverse sulfosalt families (Makovicky 1989, 1997a).

Acknowledgments

F.F. Foit Jr., P.D. Robinson, and J.R. Wilson (1995) are commended for the detailed work on the average structure of gillulyite. Assistance of A. Brask and C.H. Sarantaris in typing the manuscript and of M.B. Simonsen and B. Munch with the illustrations is gratefully acknowledged.

References cited

Balić-Žunić, T. and Makovicky, E. (1993) Contributions to the crystal chemistry of thallium sulphosalts I. The OD nature of imhofite. Neues Jahrbuch für Mineralogie, Abhandlungen, 165, 317–330.

Dittmar, G. and Schäfer, M. (1977) Darstellung und Kristallstruktur von $(NH_4)_2Sb_2S_7$. Zeitschrift für anorganische und allgemeine Chemie, 437, 183–187.

Divjaković, V. and Nowacki, W. (1976) Die Kristallstruktur von Imhofit, $Tl_{5,6}$ As_{15} $S_{25,3}$. Zeitschrift für Kristallographie, 144, 323–333.

Dornberger-Schiff, K. (1956) On the order-disorder structures (OD structures). Acta Crystallographica, 9, 593–601.

Dowty, E. (1993) ATOMS—A computer program for displaying atomic structures. IBM-PC Version 2.3, Shape Software, Kingsport.

Ďurovič, S. (1997) Fundamentals of the OD theory. European Minealogical Union Notes in Mineralogy, 1, 3–28.

Foit, F.F. Jr., Robinson, P.D., and Wilson, J.R. (1995) The crystal structure of gillulyite, $Tl_2(As, Sb)_8S_{13}$ from the Mercur gold deposit, Tooele County, Utah, U.S.A. American Mineralogist, 80, 394–399.

Guinier, A., Bokij, G.B., Boll-Dornberger, K., Cowley, J.M., Ďurovič, S., Jagodzinski, H., Krishna, P., de Wolff, P.M., Zvyagin, B.B., Cox, D.E., Goodman, P., Hahn, T., Kuchitsu, K., and Abrahams, S.C. (1984) Nomenclature of polytype structures. Report of the International Union of Crystallography Ad-Hoc Committee on the nomenclature of disordered, modulated and polytype structures. Acta Crystallographica, A40, 399–404.

Krenner, J. S. (1895) Lorandit, uj thallium-ásvány Allcharról Makedoniában. Mathematikai és Természettudományi értesitö, 13, 1895: 258–263.

Makovicky, E. (1989) Modular classification of sulphosalts—current status. Definition and application of homologous series. Neues Jahrbuch für Mineralogie, Abhandlungen, 160, 269–297.

———(1997a) Modular crystal chemistry of sulfosalts and other complex sulphides. European Mineralogical Union Notes in Mineralogy, 1, 237–271.

———(1997b) Modularity—different types and approaches. European Mineralogical Union Notes in Mineralogy, 1, 315–343.

Merlino, S., Ed. (1997) Modular Aspects of Minerals. European Mineralogical Union Notes in Mineralogy, Vol. 1. Eötvös University Press, Budapest.

Mullen, D.J.E. and Nowacki, W. (1972) Refinement of the crystal structures of realgar, AsS and orpiment, As_2S_3. Zeitschrift für Kristallographie, 136, 48–65.

Nagl, A. (1979) The crystal structure of a thallium sulphosalt Tl_8 Pb_4 Sb_{21} As_{19} S_{68}. Zeitschrift für Kristallographie, 150, 85–106.

Nakai, I. and Appleman, D.E. (1981) The crystal structure of gerstleyite $Na_2(Sb,As)_8S_{13}\cdot 2H_2O$: The first sulfosalt mineral of sodium. Chemical Letters (Japan), 1327–1330.

Parise, J.B. and Ko, Y. (1992) Novel antimony sulfides: synthesis and X-ray structural characterization of Sb_3S_5. $N(C_3H_7)_4$ and $Sb_4S_7\cdot N_2C_4H_8$. Chemistry of Materials, 4, 1446–1450.

Tan, K., Parise, J.B., Ko, Y., Dorovsky, A., Norby, P., and Hanson, J.C. (1996) Applications of synchrotron imaging plate system to elucidate the structure and synthetic pathways to open framework antimony sulfides. Abstracts XVII Congress of the International Union of Crystallography, Seattle, August 1996, PS 10.10.12:C-402.

Wilson, J.R., Robinson, P.D., Wilson, P.N., Stanger, L.W., and Salmon, G.L. (1991) Gillulyite, Tl_2 (As, $Sb)_8S_{13}$, a new thallium arsenic sulfosalt from the Mercur gold deposit, Utah. American Mineralogist, 76, 653–656.

Manuscript received April 29, 1998
Manuscript accepted September 14, 1998
Paper handled by John Parise